RSC Advances

ROYAL SOCIETY OF CHEMISTRY

www.rsc.org/advances

Graphical Abstract

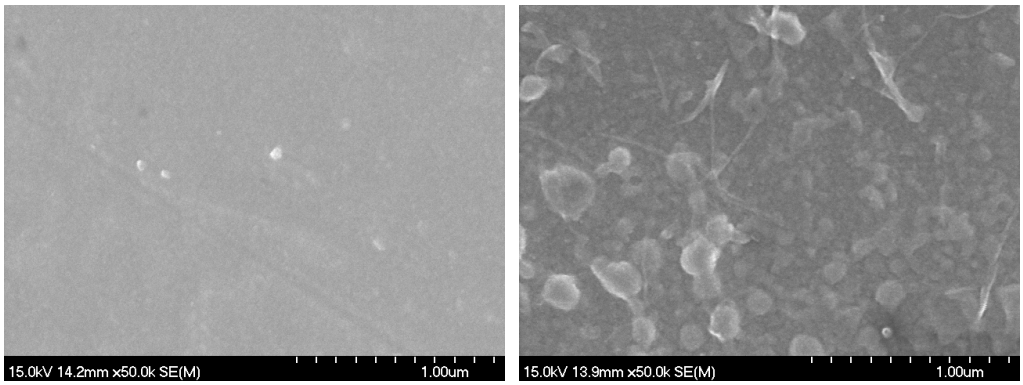

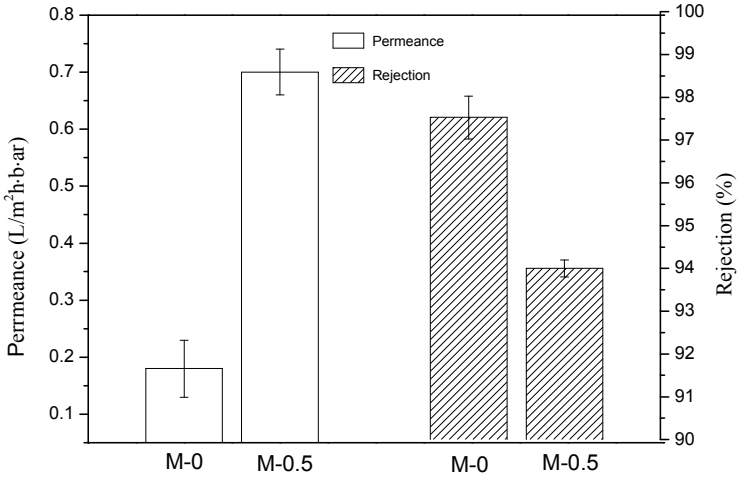

Mixed matrix membranes containing MIL-53(Al) for potential application in organic solvent nanofiltration

Lifang Zhu[a,b], Hongwei Yu[c,*], Huijuan Zhang[c], Jiangnan Shen[d,*], Lixin Xue[e], Congjie Gao[b], Bart Van der Bruggen[f]

[a] Department of Environmental Science, Zhejiang University, Hangzhou 310058, China

[b]Department of Municipal Engineering, Zhejiang University of Water Resources and Electric Power , Hangzhou 310018, China

[c]Center of Membrane Science and Water Technology, Marine College, Zhejiang University of Technology, Hangzhou 310014, China

[d]Ningbo Institute of Material Technology & Engineering, Chinese Academy of Sciences, Ningbo, 315201, P.R. China

[e]Department of Chemical Engineering, Process Engineering for Sustainable Systems (ProcESS), KU Leuven, W. de Croylaan 46, B-3001 Leuven, Belgium

Abstract:Aromatic poly(m-phenyleneisophthalamide) (PMIA) and the metal-organic framework (MOFs)MIL-53 (Al) were employed as the polymer matrix and additive, respectively, to develop mixed matrix membranes (MMMs)via non-solvent induced phase separation for potential application in organic solvent nanofiltration. The prepared membranes were characterized by scanning electron microscopy (SEM), X-ray diffraction (XRD) and water contact angle measurement. The membrane water permeance enhanced when MIL-53 (Al) was incorporated into the membrane structure while the rejection had no significant change. The optimum MMMs (with 0.5 wt.% MOFs concentration) passes mono and bivalent inorganic salts but rejects larger charged

organic molecules and has a mean effective pore size of 0.7 nm. The influence of organic solvents on MMMs performance was also investigated and the result shows that the performance shifts towards a lower pure water permeance and a higher rejection after exposure to organic solvents (ethyl acetate or methanol).The membrane performance in organic solvent nanofiltration was evaluated on the basis of the permeance and rejection of brilliant blue G in ethanol, and the result showed that the permeance of MMMs significantly increased (by 289%)while the rejection slightly reduced by 4% in contrast to the pure membrane.

Keywords: Organic solvent nanofiltration, Metal organic framework, Mixed matrix membranes, Phase inversion

1. Introduction

Nanofiltration (NF) has potential applications for separation and purification of non-aqueous mixtures (organic solvents) in food engineering, pharmaceutical processing, and petrochemical engineering, with the benefit of a low energy consumption, flexible operation and compactness of design [1]. The main challenge for organic solvent nanofiltration (OSN) membranes is that the membrane should be stable in a wide range of organic solvents and have a high and reproducible long-term performance with acceptable rejections [2].Generally, two types of polymeric membranes are used: integrally skinned asymmetric membranes, and composite membranes, which have a top layer of a different polymeric material adhered to a porous support (usually an ultrafiltration membrane). Many commercial nanofiltration membranes are fabricated by interfacial polymerization. However, the interfacial polymerization technique requires expensive manufacturing equipment. Integrally skinned asymmetric membranes can be obtained relatively

easy by phase inversion method. The desired structure can obtained by effective procedures, e.g., changing the composition in the casting solution or in the coagulation bath and in the casting conditions such as evaporating the solvent [3].

Mixed matrix membranes (MMMs) are usually formed by embedding inorganic molecular sieves, such as zeolites, SiO_2, carbon nanotubes or silicalite in a polymer matrix. The filler provides a preferential flow path for the target species [4-9]. MMMs may overcome the tradeoff between membrane permeability and selectivity, provided that defects at the filler/polymer interface can be eliminated [10-13]. To eliminate non-selective interfacial voids, surface modification of the filler is often needed to improve adhesion to the polymer matrix [14]. Recently, metal organic frameworks (MOFs) are emerging as an alternative to inorganic fillers in MMMs [15-18]. Metal organic frameworks (MOFs) are hybrid inorganic-organic solid compounds comprised of transition metals and transition metal oxides coordinated by organic linkages, often polycarboxylic acids, to create 1D, 2D, or 3D porous structures [19, 20]. These offer important advantages such as a high surface area, a relatively high thermal stability, controlled porosity, functionalizable pore walls, affinity for certain molecules, a tunable chemical composition, and flexible structure [21, 22]. The organic bridge present in the MOFs structure facilitates a better affinity for polymeric matrices than inorganic fillers, and it is easier to control MOF-polymer interactions, so that nonselective voids between the phases can be avoided [2, 18]. Numerous reports of MOFs-based mixed matrix membranes (MMMs) focused on gas separation have been published [16-18], but studies of nanofiltration are scarce [2, 23]. In the work of Basu et al. [23], the incorporation of modified MOFs in polydimethysiloxane (PDMS) membranes on a polyimide (PI) support demonstrated that

MOFs noticeably improve the retention of Rose Bengal from isopropanol due to the reduced swelling of the PDMS matrix and the size exclusion of the filler, while the permeance is not altered. Sara et al. [2] applied MOFs in a thin polyamide (PA) layer on top of cross-linked polyimide (PI) and observed that the membrane showed a dramatically increased performance without sacrificing rejection compared to unfilled membranes in MeOH/PS and THF/PS OSN experiments.

In the present work, commercial aromatic polyamides poly(m-phenyleneisophthalamide) (PMIA) and MIL-53(Al) were used as polymer matrix and filler, respectively. Aromatic polyamides have been investigated extensively as potential high-performance polymers with high thermal, chemical and thermo-oxidative stability and excellent mechanical properties, due to their crosslinked structure [24-27]. MIL-53(Al) is built of long aluminum oxide chains connected to each other by terephthalic linkers, which results in a one-dimensional structure with a channel diameter of almost 10 Å [28]. We chose MIL-53(Al) as the MOF owing to its good water stability at ambient temperature and small pore size. Besides,the carboxylic moieties at the surface of the MIL-53(Al) increase the polarity of the filler, and may thus increase the dispersability in polar media.The asymmetric membranes were prepared by non-solvent induced phase separation. The effect of adding MIL-53(Al) on the performance of PMIA membranes and the potential application in organic nanofiltration were investigated

2. Experimental

2.1. Reagents

Poly(m-phenyleneisophthalamide) (PMIA) was a commercial product (Yantai Tayho advanced materials Co., Ltd. China).The polymer was dried for at least 24 h at 100°C before being used. Its

chemical structure is shown in Fig. 1. Lithium chloride (LiCl) was of analytical grade and used after drying in a vacuum oven for approximately 24 h to 120°C. The solvent N, N-dimethylacetamide (DMAc) was of reagent grade and used as received. MIL-53(Al) was obtained from Sigma-Aldrich as Basolite A100TM, and the Al element was confirmed by XPS; this is shown in Fig S2 (Supplementary Information). Sucrose and nitroso R salt (NRS) were supplied by Huadong medicine Co. Ltd..Brilliant blue G (*M*w 854, negatively charged) was supported by Aladdin. Methanol, ethanol and ethyl acetate were of analytical grade.

2.2 Membrane fabrication

The mixed matrix membranes were fabricated via the phase inversion method, which has been described elsewhere [24]. Aromatic polyamide (PMIA) was dissolved in mixtures of lithium chloride (LiCl) and N,N-dimethylacetamide (DMAc). First, MIL-53(Al) with different concentrations (i.e., 0.3, 0.5, 1.0 and 1.5 wt.% relative to dryweight of membrane) was dispersed into DMAc/LiCl by sonication for 20 min, then 10% of the total added amount of dried PMIA fiber was added to the suspension and stirred until completely dissolved. The gradual addition of the PMIA fiber to the mixture could prevent agglomeration of both the MIL-53(Al)particle and the PMIA fiber. The remaining 90% of PMIA fiber was then added, and the mixture was stirred at least overnight. Air bubbles were removed from the suspensions by vacuum treatment. The casting solution was then cast on a clean glass plate with a knife 250 μm thick. Subsequently, the initial formed membranes were exposed in a closed vacuum oven (under the normal pressure) at 120 °C for15 min and then immersed in a deionized water coagulation bath (25± 2°C) to induce phase inversion and to form the asymmetric structure of the membranes. The fabricated membranes were

stored in fresh water for 24 h to remove any residual solvent before characterization. The fabricated MMMs were denoted as M-0.3, M-0.5 M-1.0 and M-1.5, according to the weight percentage of MIL-53(Al). The neat PMIA membrane with 0% MIL-53(Al)was fabricated as the blank membrane and was denoted as M-0. The composition of the casting solutions are shown in Table 1.

2.3 Membrane characterization

Scanning electron microscopy (SEM, HITACHI, S4700 A) was used to characterizeMIL-53(Al)and membrane morphology. The membrane was cryogenically fractured in liquid nitrogen and then coated with gold.

The static water contact angle was measured using a contact angle measurement instrument (JC-2000C1).Generally, the smaller the contact angle, the better the hydrophilicity of the membrane, which is in favor of improving the membrane permeance [29]. Deionized water, as the probe liquid, was dropped on the surface of the membrane sample at five random locations, and the average value was recorded.

XRD measurements were carried out on an X'Pert PRO X-raydiffractometer (PANalytical). A continuous scan mode with counting time 38.1 s and step size 0.0334 nm was used to collect 2θ data from 5° to 80°.

The zeta potential (ζ) was measured using a streaming potential analyzer (Zhejiang Circle-tech Membrane Technology Co., Ltd, China) [30]. Two membrane samples separated by a spacer were loaded into the clamping cell, creating a channel for electrolyte flow. The background electrolyte used for all the experiments was a 1 mM KCl solution. The temperature of the solution was maintained at 20 ^{o}C.

2.4 Membrane performance

Nanofiltration experiments were performed in a cross-flow filtration apparatus (Fig. 2). The filtration cell had an effective area of 19.6 cm^2. Before the test, all the membranes were pressurized at 10 bar with pure water for 1 h to get a stable flux, and then measured at 10 bar pressure. The flux ($L/m^2 \cdot h$) and rejection (R) are defined as:

$$F = \frac{V}{At} \quad (1)$$

$$R = \left(1 - \frac{Cp}{Cf}\right) \times 100\% \quad (2)$$

where V denotes the water volume (mL) collected during the time t (h), A is the effective membrane area forwater permeation. C_f and C_p represent feed and permeate concentrations, respectively. The concentration of sucrose was analyzed by a high performance liquid chromatography system (HPLC, Shimadzu) equipped with an XAmide NH_2columm (250 × 4.6 mm) and RI detector (Shimadzu RI-10A). The concentrations of nitroso R salt (NRS) and brilliant blue G were analyzed with a UV–Visible Spectrophotometer (UV-7502 C, Shanghai Xinmao instrument Co., Ltd., China) at a wavelength of 370 nm and 595nm, respectively.The analysisof PEG with the UV–Visible Spectrophotometer was shown in Fig S1 (Supplementary Information). The concentration of salt in the feed and permeate solutions were analyzed using electrical conductivity (Mettlertoledo). The reported values of F and R are the average of at least three replicates.

3. Results and discussion

3.1 Membrane characterization

The XRD patterns of the M-0 and M-1.5 are given in Fig 3. Compared to M-0, the new appearance of reflections at 2θ = 8.8º and 9.3º in M-0.5 correspond to the crystal structure of MIL-53(Al), which confirmed that theMIL-53(Al) crystal structure does not change after the MIL-53(Al) was successfully embedded into the polymeric membrane. With a lower loading amount of MIL-53(Al), the characteristic reflections of MIL-53(Al) in M-1.5 are relatively weaker, and even some of them are not visible. To further confirm the conclusion, we prepared a membrane with a relatively high loading (5% wt), that is M-5, and its spectrum is presented in Fig 3c. Except for the obvious reflections around 8.8 and 9.3º, other reflections corresponding to MIL-53(Al) are also observed.

Fig.4 (a) shows the SEM image of the MIL-53(Al) that was used as filler material; the particle size (< 100 nm) was observed. The SEM photograph of the M-0 and M-1.5 are shown in Fig. 4(b) and (c). White arrows point to MIL-53(Al) on the membrane surface. It can be seen that a dense skin layer was obtained.

.

SEM photographs of the membrane cross-sectionare shown in Fig. 5 (left). All membranes formed by immersion precipitation in water have an asymmetric structure with a thin dense skin layer and sponge-like sub-layer. Generally speaking, a system with a rapid phase inversion rate tends to form macrovoids with finger-like structure, whereas a system with a slow phase inversion rate results in a sponge-like structure [31]. Shu et al. reported a membrane prepared by immersing the DMAc/polyamide solution in a water bath, with macro-voids as a consequence of the complete miscibility between DMAc and water [32]. In this study, an evaporation step was used prior to

immersion in the coagulation solvent; thus, the presence of a higher polymer concentration on the surface probably increases the resistance for the exchange of solvent and non-solvent with the coagulation bath. Upon immersion of the film into the water coagulation bath, rapid solvent/nonsolvent exchange occurred. Then a relatively dense skin is formed, which slows down the diffusion of water into the polymer matrix, promoting a delayed demixing. A similar result was also observed by Huang et al. [3].

Fig. 5 (right) shows SEM images of the middle region cross-section of the pure PMIA membrane and MIL-53(Al)/PMIAmembranes. In all cases, an open cellular morphology was observed. Compared to the pure PMIA membrane, it seems that the size of the cells firstly increases and then declines for the MIL-53(Al)/PMIA composite membrane. This implies that the phase separation is initially faster and then slows down [33]. The solvent diffusion velocity from the polymer matrix can be increased by MOF addition, as a result of interactions decreasing between polymer and solvent molecules by the hindrance effect of nanofillers[34]. When the MIL-53(Al) content was further increased, the polymer casting solution became more viscous and slowed down the diffusion of water through the polymer matrix. The increasing viscosity of the casting solution acts as a physical roadblock for the mass transfer between non-solvent and solvent, leading to a delayed demixing during the membrane formation process.

As presented in Table 2, the contact angle of MIL-53(Al)/PMIA membranes decreased from 86±2°to 71±2º, which indicates that the addition ofMIL-53(Al) effectively enhances the hydrophilicity of the PMIA membrane. Two facts can be considered in order to explain this trend: Firstly, MIL-53(Al) is intrinsically hydrophilic, resulting in a natural decrease of the contact angle

of the modified membrane. Due to the addition of hydrophilic MIL-53(Al) nanoparticles, the number of hydrophilic regions on the membrane surface increases, and the affinity of the modified polymeric matrix to water molecules further improves. Furthermore, embedding with porous MIL-53(Al), the membrane surface could even become more hydrophilic due to the capability of the hydrophilic pores to imbibe water via capillary effects [35].

3.2 Characterization of membrane performance

The variation of membrane flux with theMIL-53(Al) content is shown in Fig. 6. The flux of the membrane increases with an increase in the amount of MIL-53(Al) (0-0.5 wt%). The enhancement of flux for modified membranes is thought to be caused by the increase of membrane hydrophilicity since a high hydrophilicity facilitates the solubilization and diffusion of water molecules into the membrane. In addition, the internal pores of MIL-53(Al) enhance the water permeability by providing short flow paths for water molecules. Increasing theMIL-53(Al) content further results in a small decrease in the flux of the membrane. This may be due to the aggregation of MIL-53(Al) particles at high concentrations, which would hinder a good dispersion and consequently access to the MIL-53(Al) pores [2]. It also can be seen that the permeation follows the same trend as the size of the pore, which firstly increases and then declines (see Fig. 5).

Fig. 6 also shows the rejection of MMMs depending on the organic compounds tested, i.e., sucrose and NRS. It can be seen that the sucrose and NRS rejection of the modified membrane containing various MIL-53(Al) contentwas almost unchanged compared to the pure PMIA membrane and ejections of sucrose and NRS for all membranes were over 67% and 88%, respectively. It is important to observe that sucrose and NRS have nearly the same molecular weight

(342.30 and 377.27 g/mol, respectively); however, for all the membranes, a lower rejection of sucrose than of NRS was observed. This is due to the charge effect on the separation. For sucrose, a neutral molecule, the sieving mechanism, based on the small pore size of the membrane, dominates the filtration process. The rejection of charged molecules by nanofiltration membranes, on the other hand, depends not only on the molecular size but also on the charge interactions between membrane and solution [36-38]. Above all, the optimal value for membrane performance was attained for M-0.5 membrane. The behavior of PMIA membranes is that of a negatively charged membrane, which was also proven in Fig. 7. From the results, the isoelectric point of M-0.5 was found to be at pH 3.9. The membranes are negatively charged at pH >3.9. At pH values below 3.9, the membrane is positively charged due to the adsorption of H^+. M-0.5 was also tested for filtration of Na_2SO_4 and NaCl solutions and the rejection of different solutes follow the order of Na_2SO_4 (37±1%) > NaCl (9±1%). Negatively charged membranes have a stronger repulsive force to the divalent SO_4^{2-} than to the monovalent Cl^-. Furthermore, the radius of hydrated SO_4^{2-} ions (3.0 Å) is larger than that of hydrated Cl^- ions (2.0Å) [39]. Therefore, SO_4^{2-} ions face more resistance than Cl^- ions when penetrating through the membrane. The results imply that the membrane passes mono and bivalent inorganic salts but rejects larger charged organic molecules.

The M-0.5 membrane pore sizedistribution, molecular weight cut-off (MWCO) and mean effective pore radius (r_p) were determined by the average rejections of neutral solutes using a method described elsewhere [40]. Different molecular weights of PEG were used in this study. The MWCO is defined as the molecular weight of a solute that is 90% rejected by the membrane, r_p is equal to the radius of the solute at R=50%, and σ_p , geometric standard deviation， is the solute radius ratio at

R = 84.13% over that at50%. Then the pore size distribution of the membrane can be expressed as follows:

$$\frac{dR(r_p)}{dr_p} = \frac{1}{r_p \ln\sigma_p \sqrt{2\pi}} \exp\left[-\frac{(\ln r_p - \ln \mu_p)^2}{2(\ln\sigma_p)^2}\right] \quad (3)$$

where r_p is the effective pore radius of the membrane.μ_p is thegeometric mean radius of solute at R = 50% .The values ofμ_p and σ_p determine the position and sharpness of the distribution curves, respectively. The relationship between Stokes radius r_s and M_w established for neutral solutes can be fitted by the following expression [41]:

$$\log r_s = -1.4854 + 0.4611 \log M_W \quad (4)$$

where r_s is in nm and Mw is in g/mol. From this equation the radius for a hypothetical solute at a given Mw can be obtained.

Fig. 8shows the pore size and pore size distribution curves of the M-0.5 membrane. The relationship of solute rejection against solute Stokes radius are plotted on a log-normal probability ,as illustrated in Fig.8a, Linear relationships are obtained with reasonable high correlation coefficients (R^2> 0.97).The mean effective pore radius μ_p and the geometric standard deviation σ_p, calculated from theplots , are 0.7 nm and 1.33 nm, respectively. The membrane has a mean effective pore size of 0.7 nm in radius and the MWCO of 1815 Da calculated from the fitted straight line and Eq.(4). The probability density function curves calculated from Eq. (3) are presented in Fig. 8b.The membrane has a narrow pore size distribution with most pore radius falling in between 0.4 nm and 1.1 nm. The results appear to confirm the low rejection to mono and bivalent inorganic salts, as the pore size is larger than the radius of hydrated ions.

3.3 Membrane performance in organic solvent

3.3.1Influence of organic solvent on MMMs membranes performance

The change inwaterpermeanceand of the rejection of NRS in aqueous solution after exposure of the membranes to organic solventwas investigated. M-0.5 membranes were chosen, which were exposed during 10 days to either ethyl acetate or methanol. The pure water permeance and NRS rejection were measured before and after exposure to the organic solvent. As shown in Table 3, it can be seen that the organic solvent effects the membrane performance. The water permeancedecreases after exposure to the organic solvent, while the rejection increases. This could be due to the reorganization of the polymer chains [42]. According to Ebert et al. reported [43], when a porous membrane swells, the pores become narrower, thus the membrane becomes less open, which results in higher rejection.On the other hand, for dense membranes, the polymeric chains move further apart during swelling, thus increasing the free volume; the membrane becomes more open, resulting in lower rejections Thus the nanopores on the surface shrink and the permeance declines while the rejection increases. Buonomenna et al. also reported the effect of hydratation/solvation of the membrane pore walls (smaller pore size),which decreases the pore size when hydrophilic membranes are exposed to an organic solvent [44].

3.3.2OSN results for MMMs membranes

Membrane performance in organic solvent nanofiltration was evaluated on the basis of the permeances and rejection of brilliant blue G in ethanol. All the membranes were immersed in pure ethanol for at least 48 h to reach swollen equilibrium before OSN experiments.Fig.9 shows the permeance and rejectionof membrane M-0 and M-0.5, respectively. It is noted that a remarkable

enhancement in permeance obtained for membrane M-0.5. Compared to the pure membrane (M-0),membrane M-0.5 permeance increased 289%, from 0.2 $L/m^2 \cdot h \cdot bar$ up to $0.7L/m^2 \cdot h \cdot bar$, while the rejection slightly reduced (by 4%), from 97 % down to 94 %. In addition, with respect to the results obtained for commercial OSN membranes (LES-90 (Nitto Denko Corporation),NF-SH (FilmTec Corporation) and Desal-DK (Desalination System Company))[45], measured in the same experimental conditions, listed in Table 4, membrane M-0.5 remarkable increase the rejection up to 4.5 times, i.e., from 20% (commercial membrane Desal-DK) to 94.%, while the permeance are comparable. This shows the huge potential of MOF-based membranes, which improves the transport properties of membranes for organic solvent nanofiltration.

4. Conclusions

PMIA MMMs with various amounts of MIL-53(Al) were developed through non-solvent induced phase separation. The prepared membranes have an asymmetric structure with a thin dense skin layer and sponge-like sub-layer. SEM and XRD confirmed that MOFs are present on the membrane surface..The optimum MMMs membrane has a narrow pore size distribution with most pore radius falling in between 0.4 nm and 1.1 nm and shows low inorganic salt rejection and higher rejection for charged organic dye molecules. The organic solvent influence membrane performance and the MMMsperformance shifted towards a lower pure water flux and a higher rejection after 10 days of exposure to either ethyl acetate ormethanol. The organic solvent nanofiltration results suggest that the MMMs permeance increased dramatically while keeping high rejections.

5.Acknowledgments

The research was supported by Natural Science Foundation of Zhejiang Province (No. LY12B06008), the Public Welfare Project of the Science and Technology Committee of ZhejiangProvince (2011C2071) and the Opening Foundation of Zhejiang Provincial Top Key Discipline.

References

[1] F.T. Minhas, S. Memon, M.I. Bhanger, N. Iqbal, M. Mujahid, Solvent resistant thin film composite nanofiltration membrane: Characterization and permeation study, Appl. Surf. Sci. 282 (2013) 887-897.

[2] S. Sorribas, P. Gorgojo, C. Tellez, J. Coronas, A.G. Livingston, High Flux Thin Film Nanocomposite Membranes Based on Metal-Organic Frameworks for Organic Solvent Nanofiltration, J. Am. Chem. Soc.135 (2013) 15201-15208.

[3] J. Huang, K.S. Zhang, The high flux poly (m-phenylene isophthalamide) nanofiltration membrane for dye purification and desalination, Desalination, 282 (2011) 19-26.

[4] R. Mahajan, R. Burns, M. Schaeffer, W.J. Koros, Challenges in forming successful mixed matrix membranes with rigid polymeric materials, J. Appl. Polym. Sci.86 (2002) 881-890.

[5] R. Mahajan, D.Q. Vu, W.J. Koros, Mixed matrix membrane materials: An answer to the challenges faced by membrane based gas separations today?, J. Chin. Inst. Chem. Eng. 33 (2002) 77-86.

[6] M.D. Jia, K.V. Peinemann, R.D. Behling, Molecular-Sieving Effect of the Zeolite-Filled Silicone-Rubber Membranes in Gas Permeation, J. Membr. Sci. 57 (1991) 289-296.

[7] M.M. Pendergast, E.M.V. Hoek, A review of water treatment membrane nanotechnologies, Energ. Environ. Sci.4 (2011) 1946-1971.

[8] T. Wang, J.N. Shen, L.G. Wu, B. Van der Bruggen, Improvement in the permeation performance of hybrid membranes by the incorporation of functional multi-walled carbon nanotubes,J. Membr. Sci.466 (2014) 338-347.

[9] J.N. Shen, H.M. Ruan, L.G. Wu, C.J. Gao, Preparation and characterization of PES-SiO2 organic-inorganic composite ultrafiltration membrane for raw water pretreatment, Chem. Eng. J. 168 (2011) 1272-1278.

[10] F.B Peng, L.Y. Lu, H.L. Sun, Y.Q. Wang, J.Q. Liu, Z.Y. Jiang, Hybrid organic-inorganic membrane solving the tradeoff between permeability and selectivity, Chem. Mater. 17(2005)6790-6796.

[11] F.B. Peng, L.Y. Lu, H.L. Sun, F.S. Pan, Z.Y. Jiang, Organic-inorganic hybrid membranes with simultaneously enhanced flux and selectivity, Ind. Eng. Chem. Res.46 (2007) 2544-2549.

[12] J. Ahn, W.-J. Chung, I. Pinnau, M.D. Guiver, Polysulfone/silica nanoparticle mixed-matrix membranes for gas separation, J. Membr. Sci.314 (2008) 123-133.

[13] M.Y. Kariduraganavar, J.G. Varghese, S. K. Choudhari, R. H. Olley, Organic-inorganic hybrid membranes solving the trade-off phenomenon between permeation flux and selectivity in pervaporation,Ind. Eng. Chem. Res, 48 (2009) 4002–4013.

[14] I.F.J. Vankelecom, S. VandenBroeck, E. Merckx, H. Geerts, P. Grobet, J.B. Uytterhoeven, Silylation to improve incorporation of zeolites in polyimide films, J. Phys. Chem. 100 (1996) 3753-3758.

[15] R. Zhang, S. Ji, N. Wang, L. Wang, G. Zhang, J.R. Li, Coordination-driven in situ self-assembly strategy for the preparation of metal-organic framework hybrid membranes, Chem. Int. Ed.53 (2014) 9775-9779.

[16] R. Adams, C. Carson, J. Ward, R. Tannenbaum, W. Koros, Metal organic framework mixed matrix membranes for gas separations,MicroporousMesopororous Mater. 131 (2010) 13-20.

[17] J. Ploegmakers, S. Japip, K. Nijmeijer, Mixed matrix membranes containing MOFs for ethylene/ethane separation—Part B: Effect of Cu3BTC2 on membrane transport properties, J. Membr. Sci.428 (2013) 331-340.

[18] J. Ploegmakers, S. Japip, K. Nijmeijer, Mixed matrix membranes containing MOFs for ethylene/ethane separation Part A: Membrane preparation and characterization,J. Membr. Sci. 428 (2013) 445-453.

[19] J.L.C. Rowsell, O.M. Yaghi, Metal–organic frameworks: a new class of porous materials, MicroporousMesopororous Mater. 73 (2004) 3-14.

[20] H. Li, M. Eddaoudi, M. O'Keeffe, O.M. Yaghi, Design and synthesis of an exceptionally stable and highly porous metal-organic framework, Nature, 402 (1999) 276-279.

[21] O.M. Yaghi, H.L. Li, C. Davis, D. Richardson, T.L. Groy, Synthetic strategies, structure patterns, and emerging properties in the chemistry of modular porous solids, Acc. Chem. Res. 31 (1998) 474-484.

[22] H.K. Chae, D.Y. Siberio-Perez, J. Kim, Y. Go, M. Eddaoudi, A.J. Matzger, M. O'Keeffe, O.M. Yaghi, A route to high surface area, porosity and inclusion of large molecules in crystals, Nature, 427 (2004) 523-527.

[23] S. Basu, M. Maes, A. Cano-Odena, L. Alaerts, D.E. De Vos, I.F.J. Vankelecom, Solvent resistant nanofiltration (SRNF) membranes based on metal-organic frameworks, J. Membr. Sci. 344 (2009) 190-198.

[24] N.A. Mohamed, A.O.H. Al-Dossary, Structure-property relationships for novel wholly aromatic polyamide-hydrazides containing various proportions of para-phenylene and meta-phenylene units III. Preparation and properties of semi-permeable membranes for water desalination by reverse osmosis separation performance, Eur. Polym. J.39 (2003) 1653-1667.

[25] N.A. Mohamed, Novel wholly aromatic polyamide-hydrazides .6. Dependence of membrane reverse osmosis performance on processing parameters and polymer structural variations, Polymer, 38 (1997) 4705-4713.

[26] S.H. Hsiao, M.H. He, Synthesis and properties of novel cardo aromatic poly(ether-benzoxazole)s, J. Polym. Sci. Pol. Chem.39 (2001) 4014-4021.

[27] S.C. dos Santos, L.F. Loguercio, D.S. Correa, M.R. Nunes, M.A. Villetti, I.T.S. Garcia, Interfacial properties and thermal stability of modified poly(m-phenylene isophthalamide) thin films, Surf. Interface. Anal. 45 (2013) 837-843.

[28] L. Vanduyfhuys, T. Verstraelen, M. Vandichel, M. Waroquier, V. Van Speybroeck, Ab Initio Parametrized Force Field for the Flexible Metal-Organic Framework MIL-53(Al), J. Chem. Theory Comput.8 (2012) 3217-3231.

[29] Y.X. Lv, X.H. Yu, S.T. Tu, J.Y. Yan, E. Dahlquist, Wetting of polypropylene hollow fiber membrane contactors, J Membrane Sci, 362 (2010) 444-452.

[30] J.N. Shen, C.C. Yu, H.M. Ruan, C.J. Gao, B. Van der Bruggen, Preparation and characterization of thin-film nanocomposite membranes embedded with poly(methyl methacrylate) hydrophobic modified multiwalled carbon nanotubes by interfacial polymerization, J. Membr. Sci. 442 (2013) 18-26.

[31] C.A. Smolders, A.J. Reuvers, R.M. Boom, I.M. Wienk, Microstructures in Phase-Inversion Membranes .1. Formation of Macrovoids, J. Membr. Sci.73 (1992) 259-275.

[32] S.C. Fan, Y.C. Wang, C.L. Li, K.R. Lee, D.J. Liaw, H.P. Huang, J.Y. Lai, Effect of coagulation media on membrane formation and vapor permeation performance of novel aromatic polyamide membrane, J. Membr. Sci. 204 (2002) 67-79.

[33] M.G. Buonomenna, G. Golemme, S.H. Choi, J.C. Jansen, M.P. De Santo, E. Drioli, Surface skin layer formation and molecular separation properties of asymmetric PEEKWC membranes, Sep. Purif. Technol. 77 (2011) 104-111.

[34] J.Y. Lin, R.X. Zhang, W.Y. Ye, N. Jullok, A. Sotto, B. Van der Bruggen, Nano-WS2 embedded PES membrane with improved fouling and permselectivity, J. Colloid Interf. Sci. 396 (2013) 120-128.

[35] J. Yin, E.S. Kim, J. Yang, B.L. Deng, Fabrication of a novel thin-film nanocomposite (TFN) membrane containing MCM-41 silica nanoparticles (NPs) for water purification, J. Membr. Sci. 423 (2012) 238-246.

[36] B. Van der Bruggen, J.H. Kim, F.A. DiGgiano, J. Geens, C. Vandecasteele, Influence of MF pretreatment on NF performance for aqueous solutions containing particles and an organic foulant, Sep. Purif. Technol. 36 (2004) 203-213.

[37] M.G. Buonomenna, A. Gordano, G. Golemme, E. Drioli, Preparation, characterization and use of PEEKWC nanofiltration membranes for removal of Azur B dye from aqueous media, React. Funct. Polym. 69 (2009) 259-263.

[38] B. Van der Bruggen, J. Schaep, D. Wilms, C. Vandecasteele, Influence of molecular size, polarity and charge on the retention of organic molecules by nanofiltration, J. Membr. Sci. 156 (1999) 29-41.

[39] W.P. Zhu, S.P. Sun, J. Gao, F.J. Fu, T.S. Chung, Dual-layer polybenzimidazole/polyethersulfone (PBI/PES) nanofiltration (NF) hollow fiber membranes for heavy metals removal from wastewater, J. Membr. Sci. 456 (2014) 117-127.

[40] K.Y. Wang, T.S. Chung, The characterization of flat composite nanofiltration membranes and their applications in the separation of Cephalexin, J. Membr. Sci. 247 (2005) 37-50.

[41] M.Y. Kiriukhin, K.D. Collins, Dynamic hydration numbers for biologically important ions, Biophys. Chem99 (2002) 155-168.

[42] B. Van der Bruggen, J. Geens, C. Vandecasteele, Influence of organic solvents on the performance of polymeric nanofiltration membranes, Sep. Sci. Technol. 37 (2002) 783-797.

[43] K. Ebert, F.P. Cuperus, Solvent resistant nanofiltration membranes in edible oil processing, Membr. Technol. 107 (1999) 5-8.

[44] M.G. Buonomenna, G. Golemme, J.C. Jansen, S.H. Choi, Asymmetric PEEKWC membranes for treatment of organic solvent solutions, J. Membr. Sci. 368 (2011) 144-149.

[45] Z. Xinhui, Y. Qipeng, F. Li, Y. Xiaojin, Experimental studies on transport flux and rejection for nanofiltration in organic solvents, Journal of beijing university of chemical technology (In chinese), 31 (2004) 5-8.

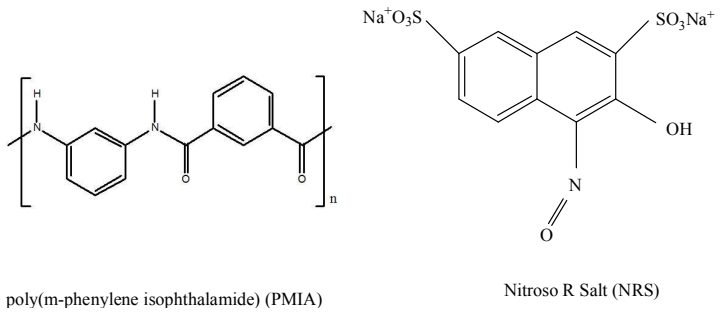

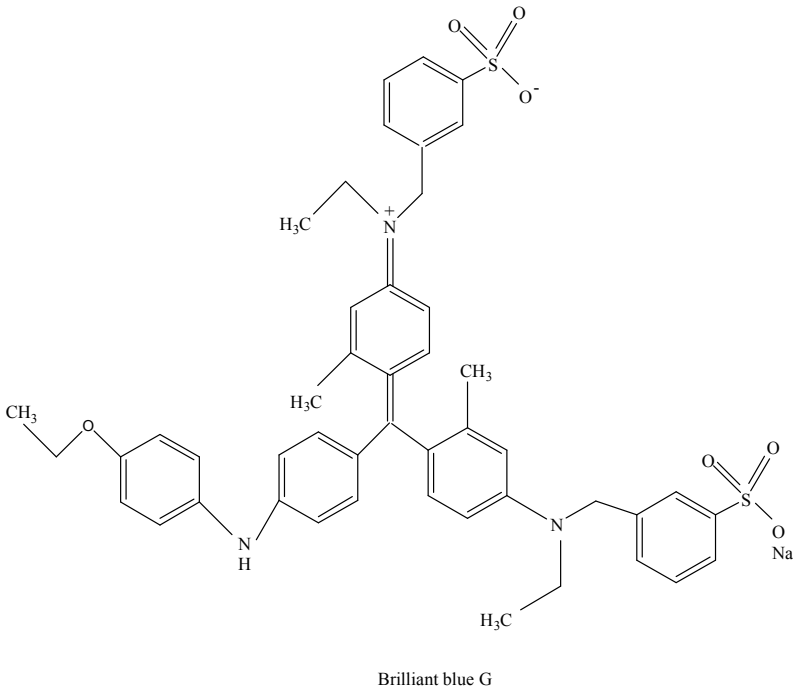

Fig.1. The structure of poly(m-phenylene isophthalamide) (PMIA), nitroso R salt (NRS) and brilliant blue G

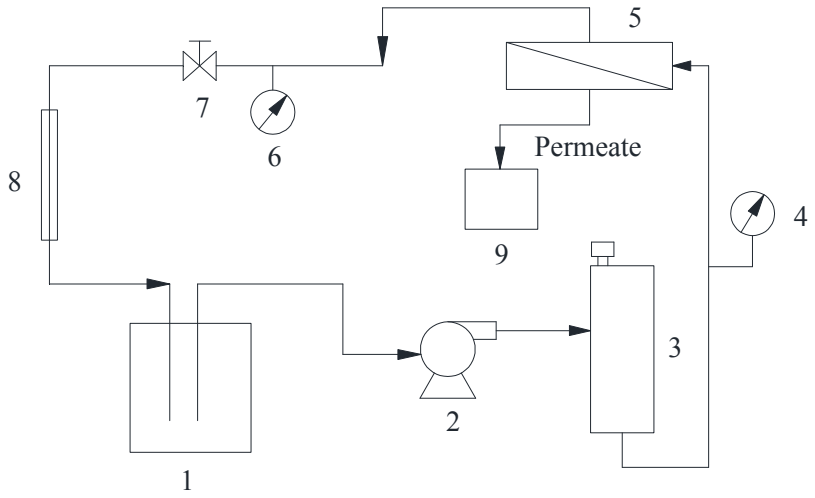

1-Feed tank; 2-Mechanical pump; 3-Buffer tank; 4-Pressure gauge; 5-Membrane module; 6-Pressure gauge; 7-Controal value; 8-Flow meter; 9-Permeate container.

Fig.2 Schematic description of membrane performance testing equipment.

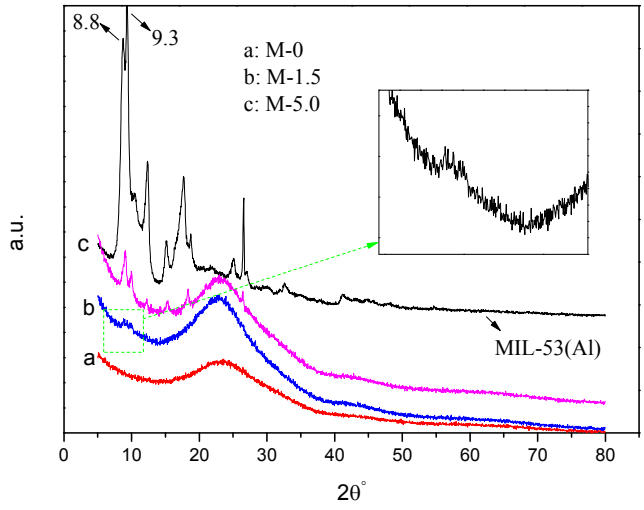

Fig.3 XRD patterns of MIL-53(Al) and MIL-53(Al) based-membranes

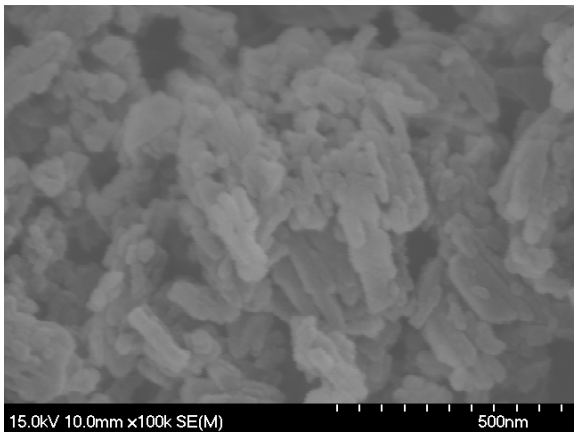

(a)

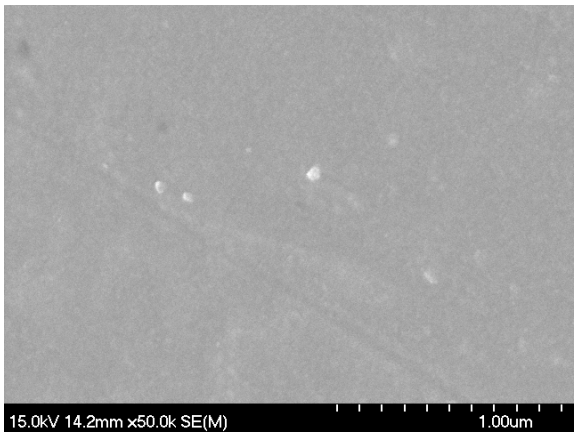

(b)

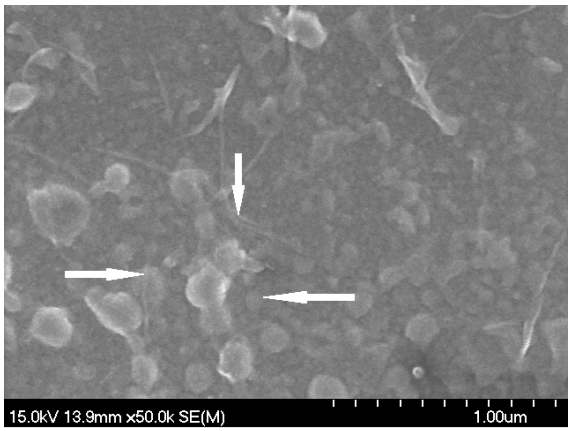

(c)

Fig. 4 SEM pictures: (a) MIL-53(Al) and skin-layer surface of MMMs with (b) 0, (c) 1.5 wt% MIL-53(Al)

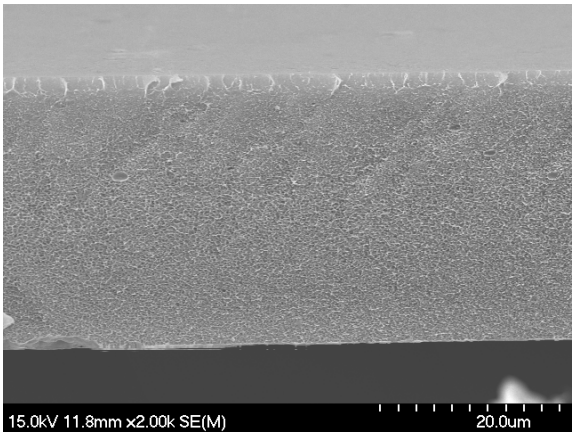

(a1)

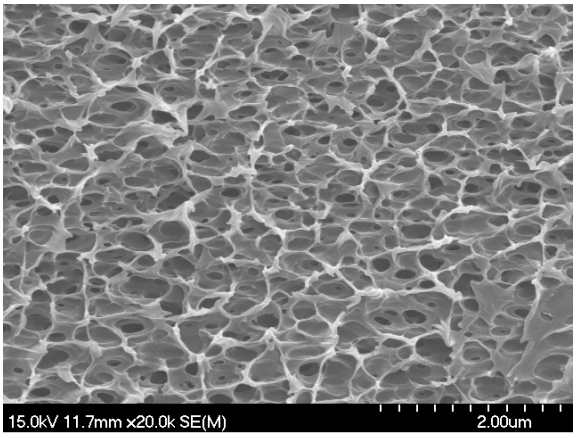

(a2)

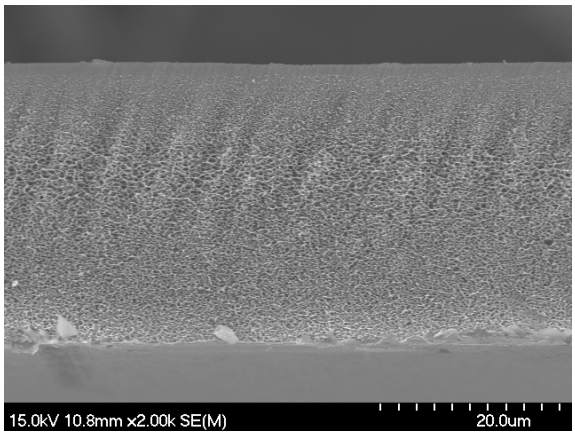

(b1)

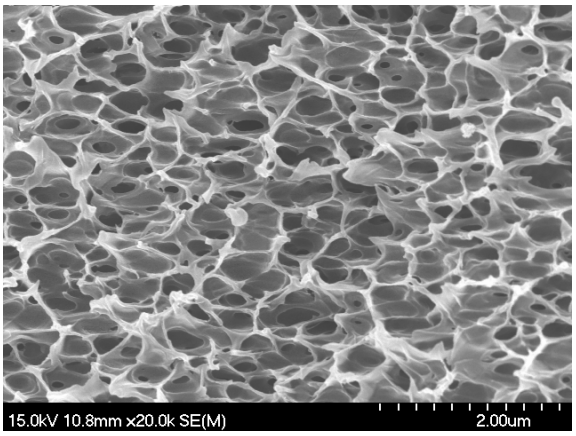

(b2)

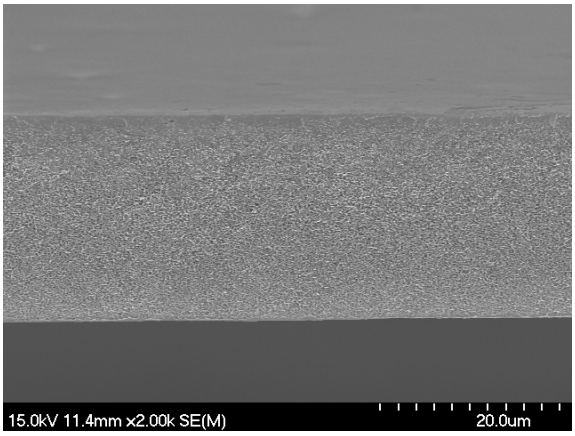

(c1)

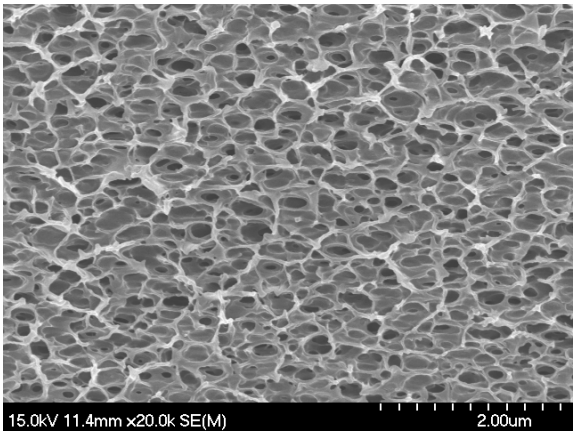

(c2)

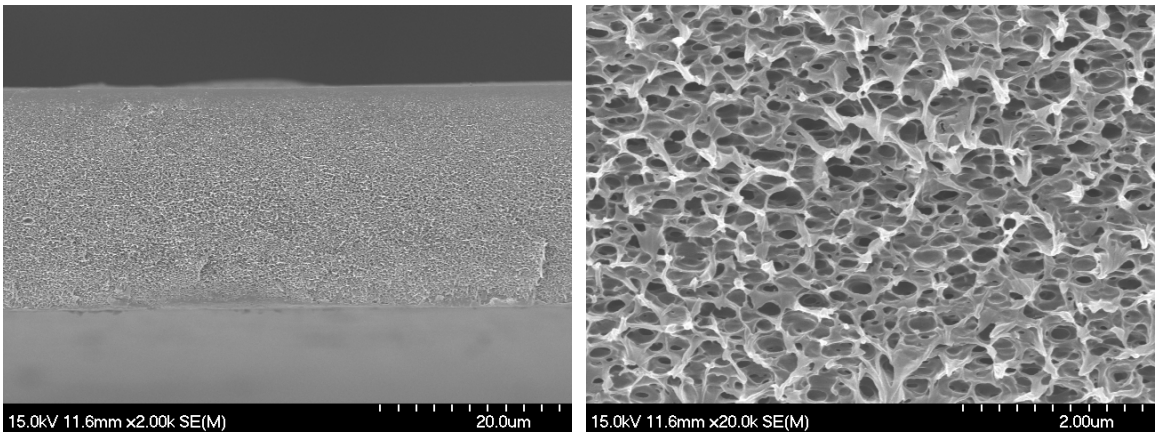

(d1) (d2)

Fig. 5 SEM images of the cross sections (left) and zoom of middle region (right) of MMMs with (a) 0, (b) 0.5, (c) 1.0 and (d) 1.5 wt% MOFs.

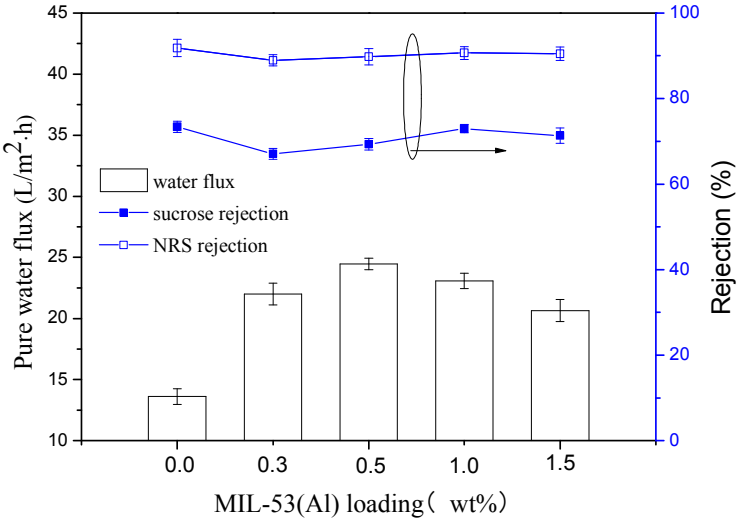

Fig. 6 Effect of MIL-53(Al) content on modified PMIA membrane performance

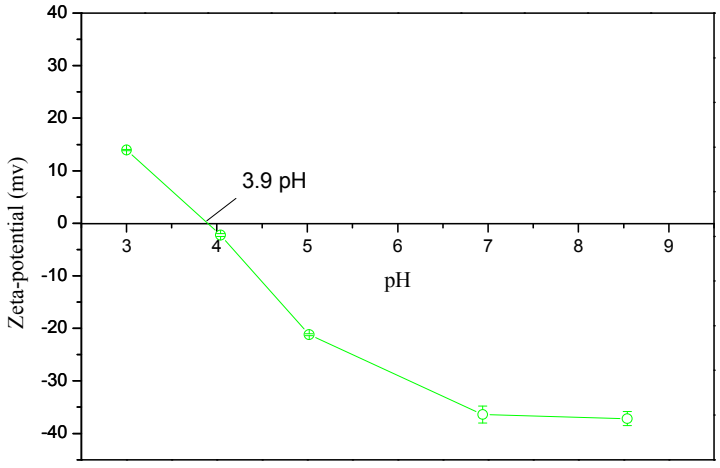

Fig. 7 The surface zeta potential as a function of pH for M-0.5

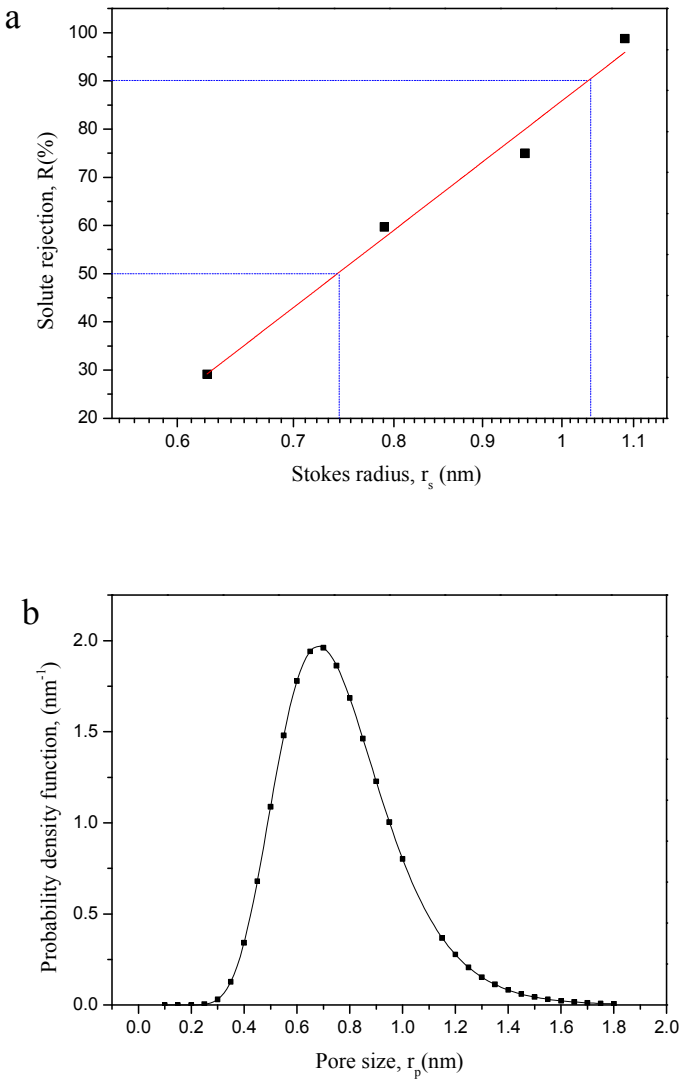

Fig. 8. (a) Log-normal probability plots of the effective rejection curve (solute rejections vs. their Stokes radii), (b) probability density function curve.

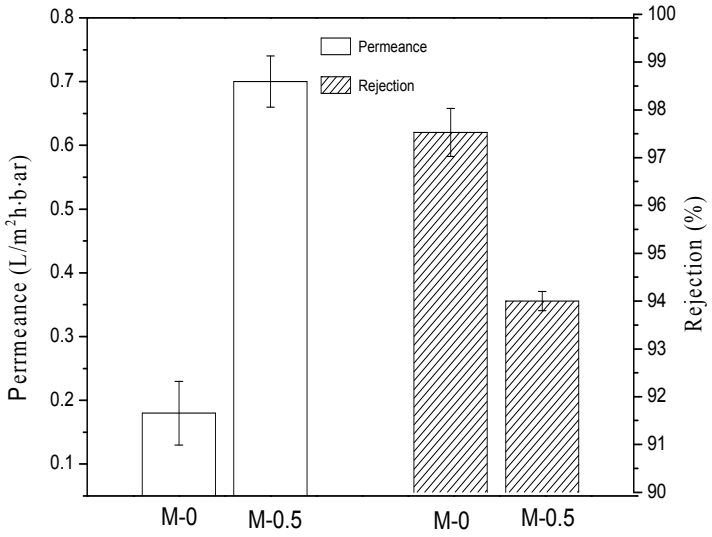

Fig. 9 Ethanol/ brilliant blue G permeances and rejections M-0 and M-0.5

Table 1 Composition of dope solution

Membrane	MOFs loading/(wt.%)	PMIA /(g)	DMAC/(g)	LiCl /(g)	MOFs/(g)
M-0	0	3	26.25	0.75	0
M-0.3	0.3	3	26.25	0.75	0.009
M-0.5	0.5	3	26.25	0.75	0.015
M-1.0	1	3	26.25	0.75	0.03
M-1.5	1.5	3	26.25	0.75	0.045

Table 2 Performance of MMMs with different MIL-53(Al) contents

MOFs content/ (wt %)	Contact angle/ (º)
0	86±2
0.3	79±2
0.5	76±1
1.0	73±1
1.5	71±2

Table 3 Water permeance and NRS rejection obtained with M-0.5 before (1) and after (2) exposure to organic solvent

Solvent	Water permeance/ ($L/m^2 \cdot h \cdot bar$)		NRS rejections/ (%)	
	(1)	(2)	(1)	(2)
Methanol	3.2	2.3	89	93
Ethyl acetate	2.8	1.9	88	92

Table 4 A comparison of brilliant blue G rejection of M-0.5 with other literature data.

Membrane	Permeance / ($L/m^2 \cdot h \cdot bar$)	Rejection/(%)
M-0.5	0.7	94
LES-90	1.1	9
NF-SH	0.6	4
Desal-DK	0.8	21